FUNDAMENTAL PHYSICAL PARAMETERS OF COLLIMATED GAMMA-RAY BURST AFTERGLOWS

A. PANAITESCU
Dept. of Astrophysical Sciences, Princeton University, Princeton, NJ 08544
AND
P. KUMAR
Institute for Advanced Study, Olden Lane, Princeton, NJ 08540

ABSTRACT

We determine the basic physical characteristics of eight Gamma-Ray Bursts (GRB) – 980519, 990123, 990510, 991028, 991216, 000301c, 000926 and 010222 – by modelling the broadband emission of their afterglows. We find that the burst kinetic energies after the GRB phase are well clustered around a mean value of 3×10^{50} ergs. In contrast, the energy release in γ-rays, after correcting for collimated explosion, varies among bursts by more than an order of magnitude. The jet initial apertures are the $2^{\rm o} - 14^{\rm o}$ range, mildly correlated with the energy, half of the jets being narrower than $\sim 3^{\rm o}$. This implies that, within 100 Mpc, there are about 10 GRB remnants (expanding at $\sim 0.1\,c$) which can be resolved with VLBA. For all eight afterglows the total energy in the shock-accelerated electrons is close to equipartition with protons. However the slope of the power-law electron distribution is not universal, varying between 1.4 and 2.8. In at least half of the cases, the density structure of the medium is inconsistent with an r^{-2} profile. A homogeneous medium with density in the $0.1 - 50$ cm^{-3} range can accommodate the broadband emission of all afterglows, with the exception of 990123, for which we find the density to be less than 10^{-2} cm^{-3}. If GRBs arise from the core collapse of massive stars, then such low densities indicate the existence of superbubbles created by the supernovae and winds within a cluster of massive stars.

1. INTRODUCTION

The detection of very energetic photons (in the GeV range) in several Gamma-Ray Bursts (GRBs) and the very short variability timescale (Fishman & Meegan 1995), sometimes less than 1 ms, exhibited by the 100 keV emission of many bursts have lead to the conclusion that they arise from sources that are moving at extremely relativistic speeds, with Lorentz factors Γ that could exceed one hundred (Fenimore, Epstein & Ho 1993, Piran 1999). Such a highly relativistic motion would follow after the release of a large amount of energy in a region of small baryonic mass. The non-uniformity in the velocity at which various parts of the outflow move leads to internal shocks. In this way a fraction of the kinetic energy of the outflow is dissipated and radiated away in γ-rays (Rees & Mészáros 1994). Some of the remaining kinetic energy is converted to electromagnetic radiation when the GRB remnant is decelerated by the circum-burst medium (Rees & Mészáros 1992). The resulting external shock energizes the swept-up gas which, similar to the GRB phase, emits synchrotron and inverse Compton emission, producing an afterglow. Theoretically, the fall-off of the afterglow Lorentz factor Γ is expected to be a power-law in the observer time, which leads to a power-law decay of the afterglow flux (Mészáros & Rees 1997). This behaviour has indeed been observed in many afterglows (e.g. Piran 1999, Piro 2000, Wheeler 2000), on timescales of days.

Due to the relativistic beaming of the emission, the observer receives radiation mostly from the fluid moving within an angle $1/\Gamma$ radians off the observer's line of sight toward the fireball center. Thus as Γ decreases, the size of the "visible" region increases. If the GRB remnant is collimated into a jet, then at some time t_j the entire jet surface becomes visible to the observer. This time is given by

$$t_j = 0.4\,(z+1)\left(E_{0,50}n_0^{-1}\right)^{1/3}\theta_{0,-1}^2\ {\rm day}\ , \qquad (1)$$

z being the burst redshift, $E_{0,50}$ the initial jet energy measured in 10^{50} erg, $\theta_{0,-1}$ its initial half-opening measured in 0.1 radians, and n_0 the external medium density in cm^{-3}. The lack of emitting fluid outside the jet opening leads to a faster afterglow decay after t_j. Furthermore, around t_j the jet starts to expand laterally (Rhoads 1999), its sweeping area increases faster than before, leading to a stronger deceleration and increasing even more the afterglow dimming rate. The most important signature produced at t_j by the jet collimation is the achromaticity of the afterglow emission break, which distinguishes it from the chromatic light-curve steepening that the passage of a spectral break through the observing band would yield. So far, there are eight well observed GRB afterglows (980519, 990123, 990510, 991208, 991216, 000301c, 000926, and 010222) for which a break or a steep decay has been observed in their optical light-curves. These are the afterglows we model in this paper.

The afterglow flux at a given frequency and time depends on the jet speed, on the properties of the external medium, and on the micro-physics of relativistic shocks. Our aim is to constrain some of these properties by modelling the afterglow dynamics, calculating its emission and using the observational data to determine $i)$ the jet energy and collimation, $ii)$ the efficiency at which relativistic shock accelerate electrons and generate magnetic fields, and $iii)$ the external medium type and density.

2. THE AFTERGLOW MODEL

There are some simplifying assumptions made in our numerical modelling, which allow the high computational speed necessary for a parameter space search. The most important simplification is that the jet front is homogeneous: the energy per solid angle and Lorentz factor have the same value in any direction within the jet aperture, and the internal energy density of the shocked fluid is uniform, at the value set by the shock jump conditions. Implicitly, we also assume that the jet has a sharp edge.

The dynamics of the jet is calculated by tracking its energy (some of which is lost radiatively), mass and aperture, which increase as the jet expands and sweeps-up the surrounding gas (Kumar & Panaitescu 2000, Panaitescu & Kumar 2000). There are only three parameters that give the jet dynamics – the initial jet energy E_0, initial half-angle θ_0, and external particle density, n for a homogeneous medium or the constant A for a wind-like medium with profile $n(r) = Ar^{-2}$.

The calculation of the afterglow synchrotron and inverse Compton emission is based on the assumption that the electron distribution $\mathcal{N}_e(\gamma)$ produced by the shock acceleration in the downstream region is a power-law $\mathcal{N}_e \propto \gamma^{-p}$ (this is supported by the observed power-law decay of many afterglows), starting from a minimum electron energy $\gamma_i m_e c^2$ and ending at a high energy break $\gamma_* m_e c^2$. The existence of this high energy break is due to the escape of particles from the acceleration region, to radiative losses, and is also required to have a finite energy in electrons if $p < 2$. For simplicity we approximate the cut-off at γ_* as a steeper power-law of index q.

There are three or five model parameters pertaining to the microphysics of shock acceleration and magnetic field generation, based on which we calculate the co-moving frame afterglow spectrum. The magnetic field strength is simply parameterized by the fraction ε_B of the post-shock energy density that resides in it. The distribution of the injected electrons is defined by the fractional energy ε_e in electrons if they all had the same $\gamma = \gamma_i$ (thus ε_e parameterizes γ_i) and the index p of the power-law distribution above γ_i. The cut-off γ_* is set by the the fractional energy ϵ of the electrons between γ_i and γ_*.

The synchrotron spectrum is piece-wise power-law, with breaks at the self-absorption frequency ν_a, injection frequency ν_i corresponding to the minimum electron γ_i, cooling frequency ν_c corresponding to an electron cooling timescale equal to the dynamical time, and cut-off frequency ν_* associated with γ_*. The afterglow spectrum and light-curve is determined by the evolution of these spectral breaks and of the flux at peak frequency $\nu_p = \min(\nu_c, \nu_i)$. We note that for a spreading jet ($t > t_{jet}$), the afterglow emission at frequencies above ν_i decays approximately as $F_\nu \propto t^{-p}$, irrespective of the location of ν_c, provided that the electron cooling is dominated by synchrotron emission. Therefore the temporal slope of the post jet-break optical or radio light-curves gives a direct measurement of the electron distribution index p.

We calculate numerically the afterglow emission for an observer lying on the jet axis, by integrating the synchrotron and inverse Compton emissions over the jet dynamics, taking into account the variation of the bulk Lorentz factor Γ on the equal arrival time surface. We note that the afterglow light-curve has a weak dependence on observer location offsets less than θ_0 . The equations we employ for the calculation of the jet dynamics and of the received radiation (Kumar & Panaitescu 2000, Panaitescu & Kumar 2000, 2001) are valid in any relativistic regime. For the parameters we find for various GRB afterglows, the non-relativistic regime should set in after the last available observations. It is the mildly relativistic regime that corresponds to observations made later than about 10 days after the GRB event, for which a numerical treatment is most appropriate.

3. FEATURES OF GRB JETS

Based on the afterglow model outlined above, we model the broadband, time-dependent emission of eight GRB afterglows: 980519, 990123, 990510, 991208, 991216, 000301c, 000926 and 010222, whose light-curves exhibited a break, offering thus the possibility of determining the initial jet opening θ_0 and energy E_0.[1] The basic afterglow parameters: E_0, θ_0, n, ε_e, ε_B, and p (as well as ϵ and q when they are relevant) are determined by minimization of χ^2 (maximization of the likelihood to obtain the observed fluxes). Figure 1 shows the data and the model light-curves in three distinct domains: radio, optical and X-ray. The averages and dispersions of parameters for our eight GRBs, calculated from the best fit parameters of individual bursts, are

$$E_0 = (2.6 \pm 1.1) \times 10^{50} \text{ erg} , \quad \theta_0 = 6.1^{\rm o} \pm 4.5^{\rm o} ,$$
$$\log(n/\text{cm}^{-3}) = 0.13 \pm 1.35 , \quad \varepsilon_e = 0.062 \pm 0.045 ,$$
$$\log \varepsilon_B = -2.4 \pm 1.2 , \quad p = 1.87 \pm 0.51 .$$

Figure 2 shows the best fit parameters and their 90% confidence levels, determined by variation of χ^2 around its minimum, for our set of eight afterglows. As illustrated, we find that jet energies that are clustered between 10^{50} and $\sim 6 \times 10^{50}$ erg,[2] somewhat smaller than the typical kinetic energy of a supernova. Thus only a very small fraction ($\sim 10^{-4}$) of the energy budget expected for GRB progenitors (Paczyński 1998, Mészáros, Rees & Wijers 1999, MacFadyen, Woosley & Heger 2001) is given to highly relativistic ejecta. It is then surprising that the variation of this fraction among bursts is merely a factor of a few.

We have found that models with a homogeneous medium can explain well the broadband emission of all eight afterglows, although in one case (000926) the best fit is unsatisfactory (χ^2 is rather large). For 980519 and 990510 we determine external particle densities around ~ 0.1 cm^{-3}, typical for warm interstellar medium, while for 991208, 991216, 000301c, 000926 and 010222 the densities we find are around 10 cm^{-3}. For 990123 we obtain an external density below 10^{-2} cm^{-3}, similar to the afterglow 980703 (Panaitescu & Kumar 2001).

Our afterglow calculations also show that an r^{-2} density profile of the external medium is compatible with the emission of 991208 and 991216, and can marginally accommodate the afterglows 000301c and 010222, but cannot explain the broadband emission of 980519, 990123, 990510 and 000926. Therefore our findings are not consistent with the "pure" winds expected from Wolf-Rayet stars (Chevalier & Li 1999) and are in accord with the results of Ramirez-Ruiz et al. (2001), who have shown that the interaction between such winds and the circumstellar medium leads to the formation of a quasi-homogeneous shell extending from $\sim 10^{16}$ cm to $\gtrsim 10^{18}$ cm.

Regarding the microphysics of shocks, the results presented in Figure 2 indicate that i) the total electron energy is close to equipartition with protons, ii) the magnetic field strength, $B \propto \varepsilon_B^{1/2}$, is within two orders of magnitude of the equipartition value, and iii) the power-law distribution of shock-accelerated electrons does not have an universal index p, with $1.4 < p < 2.8$. Given that the post jet-break emission falls-off as t^{-p}, the shallow decays of the optical emission of 010222 and radio light-curves of 991208, 991216 and 000301c require

[1] Other afterglows did not have such a break for the duration spanned by the observations. Although they may have been collimated, the initial jet angle cannot be determined without having an observational constraint on the jet break time t_j.

[2] Using the analytical expression for the jet break time, Frail et al. (2000) have calculated jet apertures θ_0 for more afterglows and found that the energies released in γ-rays by GRB jets are also clustered within a factor of 4.

models with $p \sim 1.5$. Consistency between such hard electron distributions and the observed optical spectral slopes implies that, for these four afterglows, the cooling frequency ν_c was below the optical domain.

In our modelling, the passage of a high energy spectral break ν_* yields most of the steepening of the optical decay observed in the afterglows 991208, 991216 and 000301c. This allows us to determine the fractional electron energy up to γ_* corresponding to ν_*. We find this fraction to be in the range 1/3–2/3 (Figure 2), close to equipartition, which provides a natural reason for the existence of the break at γ_*. We note that hard electron distributions and equipartition electron energies find mutual consistency in the shock acceleration treatment of Malkov (1999).

Assuming an uniform jet, the jet energies and apertures inferred here and the observed γ-ray fluences require an efficiency of the γ-ray mechanism in dissipating the jet kinetic energy and radiating it in the 20 keV–1 MeV range which exceeds $\sim 50\%$. However if the γ-ray emission arises from bright patches caused by angular fluctuations (Kumar & Piran 2000) of the kinetic energy on the jet surface, the actual efficiency can be much smaller, closer to that obtained from numerical modelling of internal shocks (Spada, Panaitescu & Mészáros 2000). These bright spots could also induce short timescale fluctuations in the early X-ray and optical afterglow emission, before these fluctuations disperse, and may have already been observed in the optical light-curve of 000301c.

4. CONCLUSIONS

The findings reported above should shed some light on the GRB progenitors. Homogeneous media of low density, below $10^{-2}\ \mathrm{cm}^{-3}$, as found for the afterglows 990123 and 980703, indicate a galactic halo or a hot component of the interstellar medium. External particle densities in the $0.1 - 1\ \mathrm{cm}^{-3}$ range, as found for 980519 and 990510, are characteristic for the interstellar medium, while larger values of $\sim 10\ \mathrm{cm}^{-3}$, as determined for the afterglows 991208, 000301c, 000926, and 010222, are typical for diffuse hydrogen clouds. Even larger particle densities, above $100\ \mathrm{cm}^{-3}$, would be consistent with the undisturbed, dense molecular clouds expected in the currently popular collapsar model (Woosley 1993, Paczyński 1998, MacFadyen & Woosley 1999) for GRB progenitors. Scalo & Wheeler (2001) have emphasized that the winds and supernovae occurring in a cluster of massive stars create 10 pc–1 kpc superbubbles whose density can be as low as $10^{-3}\ \mathrm{cm}^{-3}$. Furthermore they argued that variations in the cluster age and the density of the giant molecular cloud into which the superbubble expands, as well as the interaction with the winds from other clusters, may yield circumburst medium densities spanning a few orders of magnitude.

The relativistic kinetic energies of the eight GRBs analyzed here show a remarkably narrow distribution, with mean value of $\sim 3\times10^{50}$ erg and dispersion of $\sim 10^{50}$ erg. On the other hand, the distributions of the γ-ray energy output (assuming uniform jets) and of the jet initial aperture are significantly broader, with a width of one order of magnitude.

That half of the afterglows analyzed here are narrower than $\sim 3^{\rm o}$ (Figure 2), indicates that the distribution of initial jet angles is dominated by very narrow jets.[3] Taking into account that star formation rate at redshift $z \sim 1$ was an order of magnitude larger than at present (Madau, Pozzetti & Dickinson 1998), the rate of collimated GRBs is $\gtrsim 10^3$ times smaller than that of supernovae. As pointed out by Paczyński (2001), if the fraction of core collapse supernovae associated with GRBs is at $z \sim 1$ the same as in the nearby Universe then, within 100 Mpc, there should be $\lesssim 10$ GRB remnants that are sufficiently bright and large after several years to allow the resolution of their nonspherical structure with VLBA. These remnants will have typical velocities of $0.1\,c$, therefore the expansion of the nearest remnants, over several years, could be detectable.

From the afterglow parameters presented in Figure 2, one can show that the jet Lorentz factor at the end of the GRB phase is 160 ± 70. For the typical jet energy given above, this implies that the baryonic mass ejected at ultra-relativistic speeds by the GRB explosion is about $10^{-6} M_\odot$. If the GRB progenitor is a $10\,M_\odot$ star, the largest jet apertures ($\sim 10^{\rm o}$) and the baryonic loads determined here imply that the region of the star through which the jet propagates is evacuated up to 1 part in 10^5.

Our calculations led the surprising result that the electron energy distribution index varies significantly among GRB afterglows, suggesting that the details of the acceleration of particles at ultra-relativistic shocks are not universal. We also find that the energy imparted to electrons at relativistic shocks should be close to equipartition with protons.

AP acknowledges the supported received from Princeton University through the Lyman Spitzer, Jr. fellowship. PK was supported in part by the Ambros Monell foundation and NSF grant Phy-0070928. We thank Bohdan Paczyński, John Scalo and Craig Wheeler for helpful comments.

REFERENCES

Chevalier, R. & Li, Z. 1999, ApJ, 520, L29
Fenimore, E., Epstein, R. & Ho, C. 1993, A&AS, 97, 59
Fishman, G. & Meegan, C. 1995, ARA&A, 33, 415
Frail, D. et al. 2001, ApJL, submitted (astro-ph/0102282)
Goodman, J. 1997, New Astronomy, 2, 449
Kumar, P. & Piran, T. 2000, ApJ, 535, 152
Kumar, P. & Panaitescu, A. 2000, ApJ, 541, L9
MacFadyen, A., Woosley, S. & Heger, A. 2001, ApJ, 550, 410
MacFadyen, A., & Woosley, S. 1999, ApJ, 524, 262
Madau, P., Pozzetti, L. & Dickinson, M. 1998, ApJ, 498, 106
Malkov, M. 1999, ApJ, 511, L51
Mészáros, P. & Rees, M.J. 1997, ApJ, 476, 232
Mészáros, P., Rees, M.J. & Wijers, R. 1999, New Astronomy, 4, 303
Paczyński, B. 1998, ApJ, 494, L45
Paczyński, B. 2001, Acta Astronomica, 51, 1
Panaitescu, A. & Kumar, P. 2000, ApJ, 543, 66
Panaitescu, A. & Kumar, P. 2001, ApJ, 554, 667
Piran, T. 1999, Phys. Rep., 314, 575
Piro, L. 2000, Proceedings of "X-ray Astronomy '99: Stellar Endpoints, AGN and the Diffuse X-ray Background", ed. N. White, Bologna (astro-ph/0001436)
Ramirez-Ruiz, E., Dray, L., Madau, P. & Tout, C. 2001, MNRAS, submitted (astro-ph/0012396)
Rees, M.J. & Mészáros, P. 1992, MNRAS, 258, 41p
Rees, M.J. & Mészáros, P. 1994, ApJ, 430, L93
Rhoads, J. 1999, ApJ, 525, 737
Scalo, J. & Wheeler, J. 2001, ApJ, submitted (astro-ph/0105369)
Spada, M., Panaitescu, A. & Mészáros, P. 2000, ApJ, 537, 824
Wheeler, J.C. 2000, "The Largest Explosions since the Big Bang: Supernovae and GRBs", eds. M. Livio, K. Sahu & N. Panagia, Cambridge: Cambridge University Press (astro-ph/9909096)
Woosley, S. 1993, ApJ, 405, 273

[3] Admittedly, our criterion for selecting the eight cases analyzed here excludes some well observed afterglows for which an optical light-curve break was not seen. Such afterglows should arise from wider jets, most likely with $\theta_0 \gtrsim 20^{\rm o}$.

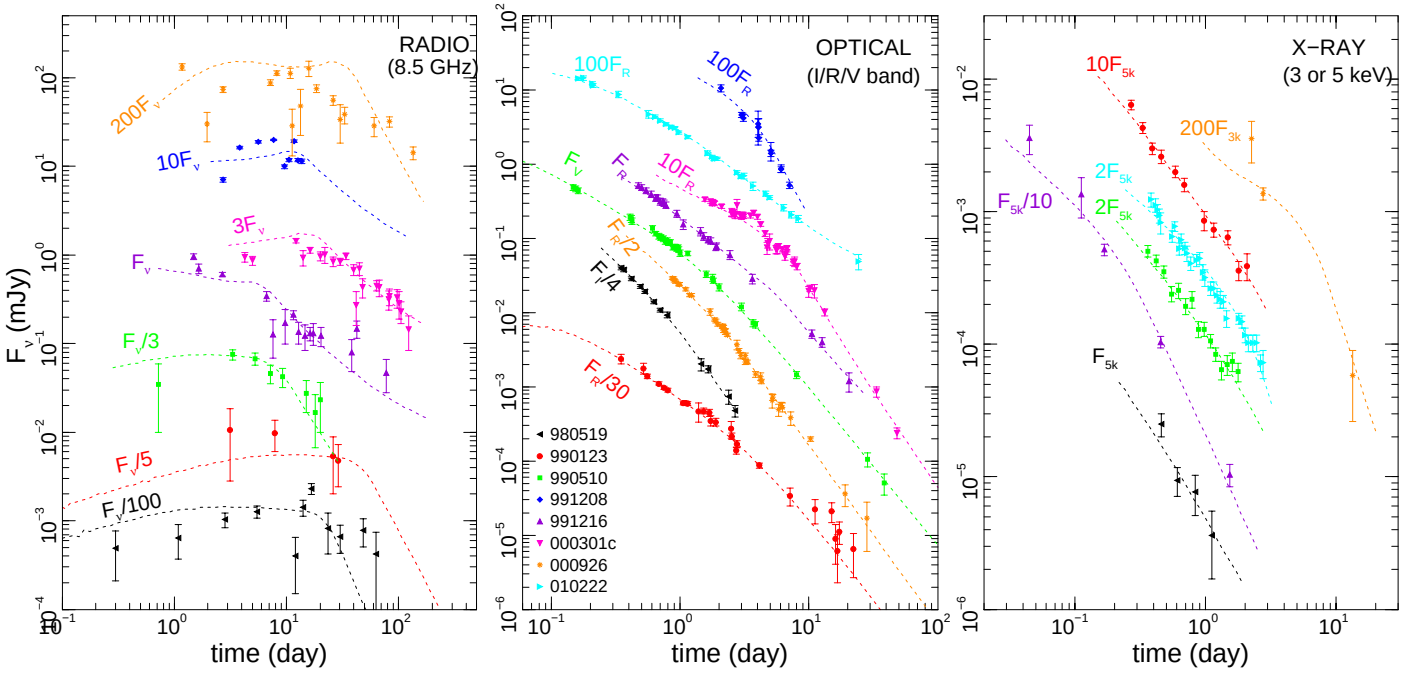

FIG. 1.— Radio, optical and X-ray emission and model light-curves for the GRB afterglows 980519, 990123, 990510, 991208, 991216, 000301c, 000926, and 010222 (legend of middle graph applies to all panels). The numerical light-curves have been obtained by minimization of χ^2 between model emission and the radio, millimeter, sub-millimeter, near infrared, optical, and X-ray data (only a part of the used data is shown in this figure). The parameters of each model are given in *Figure 2*. Optical data has been corrected for Galactic dust extinction. The spread around the model curves exhibited by the radio emission of 980519, 991208, 991216, 000301c and 000926 can be explained by fluctuations due to scatterings by the inhomogeneities in the Galactic interstellar medium (Goodman 1997). Fluxes have been multiplied by the indicated factors, for clarity.

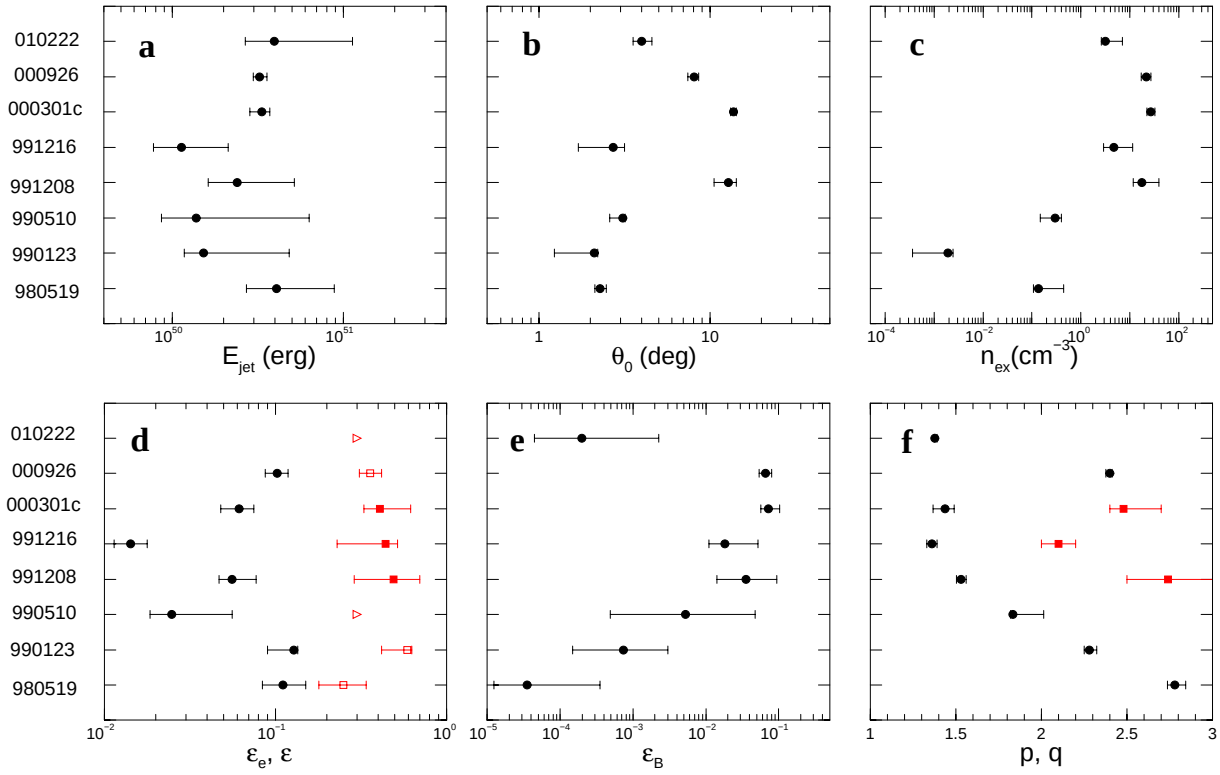

FIG. 2.— Best fit model parameters and their 90% confidence intervals for the afterglows shown in *Figure 1*. **a**: jet initial energy E_0, **b**: initial half-angle θ_0, **c**: external medium density n, **d**: parameter ε_e for minimum injected electron energy (filled circles), fractional electron energy ϵ up to the γ_*-break (filled squares, triangles indicating lower limits), and the total electron energy $\frac{p-1}{p-2}\,\varepsilon_e$ if the electron distribution extends to infinity (open squares), **e**: magnetic field parameter ε_B, **f**: index p of the power-law injected electron distribution (filled circles), and index q above the γ_*-break (filled squares). For 010222 we find an unusually small $\varepsilon_e = 0.2^{+2.1}_{-0.1} \times 10^{-3}$.